J|A|C|S
ARTICLES
Published on Web 06/17/2003

Structural, Spectroscopic, and Redox Consequences of a Central Ligand in the FeMoco of Nitrogenase: A Density Functional Theoretical Study

Timothy Lovell,* Tiqing Liu, David A. Case,* and L. Noodleman*

Contribution from the Department of Molecular Biology TPC-15, The Scripps Research Institute, La Jolla, California 92037

Received March 11, 2003; E-mail: case@scripps.edu

Abstract: Broken symmetry density functional and electrostatics calculations have been used to shed light on which of three proposed atoms, C, N, or O, is most likely to be present in the center of the FeMoco, the active site of nitrogenase. At the $Mo^{4+}4Fe^{2+}3Fe^{3+}$ oxidation level, a central N^{3-} anion results in (1) calculated Fe−N bond distances that are in very good agreement with the recent high-resolution X-ray data of Einsle *et al.*; (2) a calculated redox potential of 0.19 eV versus the standard hydrogen electrode (SHE) for FeMoco-(oxidized) + $e^- \rightarrow$ FeMoco(resting), in good agreement with the measured value of −0.042 V in *Azotobacter vinelandii*; and (3) average Mössbauer isomer shift values ($IS_{av} = 0.48$ mm s^{-1}) compatible with experiment ($IS_{av} = 0.40$ mm s^{-1}). At the more reduced $Mo^{4+}6Fe^{2+}1Fe^{3+}$ level, the calculated geometry around a central N^{3-} anion still correlates well with the X-ray data, but the average Mössbauer isomer shift value ($IS_{av} = 0.54$ mm s^{-1}) and the redox potential of −2.21 eV show a much poorer agreement with experiment. These calculated structural, spectroscopic, and redox data indicate the most likely iron oxidation state for the resting FeMoco of nitrogenase to be $4Fe^{2+}3Fe^{3+}$. At this favored oxidation state, oxygen or carbon coordination leads to (1) Fe−O distances in poor agreement and Fe−C distances in good agreement with experiment and (2) calculated redox potentials of +0.97 eV for O^{2-} and −1.31 eV for C^{4-}. The calculated structural parameters and/or redox data suggest either O^{2-} or C^{4-} is unlikely as a central anion.

1. Introduction

A high-resolution X-ray crystallographic analysis of the nitrogenase MoFe protein has recently revealed a previously unrecognized ligand coordinated to six iron atoms in the center of the catalytically essential FeMo-cofactor (FeMoco).[1] The new central atom completes an approximate tetrahedral coordination for each of the six iron atoms of the prismane, instead of the quite unusual trigonal coordination originally proposed on the basis of lower resolution structures.[2] The crystallographic refinement at 1.16 Å resolution is consistent with this newly detected atomic component being a light element, most plausibly nitrogen, but unambiguous identification of the atom type based on electron density alone has proven to be difficult, even at such a high level of resolution.

Carbon, nitrogen, oxygen, and sulfur have been postulated as chemically plausible candidates for the central atom (Figure 1), and each has been tested against the available diffraction data. Of these four elements, sulfur was deemed the least likely for several reasons but primarily because the observed distances to the surrounding iron atoms were too short. Carbon, nitrogen, or oxygen could not be differentiated, nor could they be ruled out from the X-ray analysis. On the basis of the resolution-dependent electron-density profile and the fact that nitrogenase interacts with dinitrogen to generate ammonia, this central ligand was tentatively assigned as N.[1]

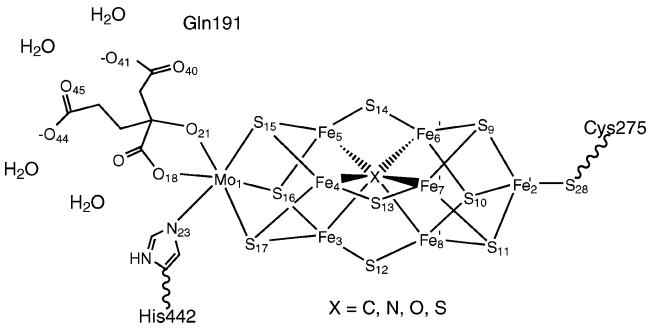

Figure 1. FeMoco of nitrogenase with an unknown ligand (X marks the spot) sitting in the center. The immediate protein environment surrounding the homocitrate is also shown.

Previously, we[3] and other workers[4] have used various theoretical approaches to examine the electronic structure of FeMoco. For the resting state of the enzyme, our focus was on the spin coupling mode within the seven iron sites, a detailed oxidation state description for the iron sites for the most stable

(1) Einsle, O.; Teczan, F. A.; Andrade, S. L. A.; Schmid, B.; Yoshida, M.; Howard, J. B.; Rees, D. C. *Science* **2002**, *297*, 1696.
(2) (a) Kim, J.; Rees, D. C. *Nature* **1992**, *360*, 553. (b) Kim, J.; Rees, D. C. *Science* **1992**, *257*, 1677. (c) Chan, M. K.; Kim, J.; Rees, D. C. *Science* **1993**, *260*, 792. (d) Georgiadis, M. M.; Komiya, H.; Woo, D.; Kornuc, J. J.; Rees, D. C. *Science* **1992**, *257*, 1653. (e) Kim, J.; Woo, D.; Rees, D. C. *Biochemistry* **1993**, *32*, 7104. (f) Bolin, J. T.; Ronco, A. E.; Morgan, T. V.; Mortenson, L. E.; Xuong, N. *Proc. Natl. Acad. Sci. U.S.A.* **1993**, *90*, 1078. (g) Mayer, S. M.; Lawson, D. M.; Gormal, C. A.; Roe, S. M.; Smith, B. E. *J. Mol. Biol.* **1999**, *292*, 871. (h) Schindelin, N.; Kisker, C.; Schlessman, J. L.; Howard, J. B.; Rees, D. C. *Nature* **1997**, *387*, 370. (i) Strop, P.; Takahara, P. M.; Chiu, H.-J.; Angove, H. C.; Burgess, B. K.; Rees, D. C. *Biochemistry* **2001**, *40*, 651.

spin coupling mode for the resting cofactor,[3] as well as a comparison of measured and calculated redox data in the protein environment for experimentally characterized states of the FeMoco.[3d]

The revelation that an atom sits in the center of the FeMoco[1] now introduces a major new factor compared with our previous theoretical assessment. Originally, we assigned the most likely oxidation states of the molybdenum and iron sites to be $Mo^{4+}6Fe^{2+}1Fe^{3+}$ consistent with ENDOR data,[5] but this assignment needs to be re-examined, especially in light of the alternative $Mo^{4+}4Fe^{2+}3Fe^{3+}$ oxidation states also proposed on the basis of Mössbauer measurements.[6] The presence of the newly detected central atom may also help to explain why our original redox potential calculations for the FeMoco with no central atom deviated from experiment by +0.82 V,[3d] even though, for a number of iron−sulfur clusters in proteins, our calculated redox potentials are generally 0.2 to 0.3 eV lower than experiment.[7] In this work, for the two postulated sets of metal-ion valencies, we now examine how the presence of a centrally located atom affects three calculated properties for the active site of nitrogenase: cofactor geometry, the electron density at the iron sites, and hence, the average Mössbauer isomer shift value, and the redox potential between the resting cofactor and its one-electron oxidized counterpart in the protein environment.

2. Methods

2.1. Quantum Model of Nitrogenase Cofactor and Immediate Protein Environment. The starting geometries for the cofactor models were based on our optimized FeMoco structures for spin alignment BS6-1, with no central ligand present.[3a] A central ligand was inserted into the structure at distances comparable to those observed in the 1.16 Å structure. The model cofactors in this work (Figure 1) are composed of the [Mo7Fe9S] core, a methyl thiolate approximating the side chain ligand of Cys275, an imidazole to represent the side chain of His442, and the fully deprotonated homocitrate ligand (charge = −4). Within the first coordination shell, the central ligand has been modeled as either a C^{4-}, an N^{3-}, or an O^{2-} atom. Second shell ligands included are the side chain of Gln191 (represented by acetamide) and four structurally characterized water molecules, all of which hydrogen bond to the negatively charged oxygen ends of the homocitrate ligand.

2.2. Density Functional Calculations. All calculations employed the Amsterdam Density functional package (ADF, version 2.3)[8] to compute the geometries and energies of the active site clusters. The ADF basis set IV was used for all atoms, corresponding to uncontracted triple-ζ Slater-type orbitals (STO) for the 4s, 4p, 5s, and 4d valence orbitals of Mo, 3s, 3p, 4s, and 3d valence orbitals of Fe, triple-ζ STOs for the 2s, 2p valence orbitals of C, N, and O augmented with a 3d polarization orbital, and triple-ζ STO for 1s of H with a 2p polarization orbital.[9] Electrons in orbitals up to and including 3d {Mo}, 2p {V, Fe, S}, and 1s {N, O, C} were considered to be part of the core and treated in accordance with the frozen core approximation. The numerical integration scheme was the polyhedron method developed by the Velde *et al*.[10] For all geometry optimizations, the analytical gradient method implemented by Versluis *et al*.[11] was used with a numerical integration accuracy of 4.0. Convergence criteria were set to 0.001 Å in coordinates and 0.01 Hartree/Å in the norm of all gradient vectors. Geometry optimizations were performed using the generalized gradient correction terms including in the SCF potential (local Vosko−Wilk−Nusair (VWN) + nonlocal Becke−Perdew (BP86) for exchange and correlation).[12] Calculations were performed without symmetry using a parallel version of the ADF code on four SGI R10000 nodes.

Within the $MoFe_7S_9X$ (X = C, N, O) core, all bond lengths and angles were fully optimized, along with atoms directly ligated to the Mo (homocitrate oxygens and imidazole nitrogen) and 7Fe (cysteine sulfur) centers. The internal geometries (but not the relative positions) of coordinated protein residues within the first coordination sphere, such as the imidazole ring and the methyl component of the methyl thiolate group, were constrained to their X-ray values, as described previously. Second shell ligands were given all degrees of freedom, allowing for the possible transfer of protons between the unsaturated oxygens of the homocitrate and the second shell hydrogen-bonding ligands (Gln191 and 4 waters) to occur.[13]

To describe spin polarization and spin coupling, the calculations were done with the spin-unrestricted broken-symmetry (BS) approach described many times before.[14] To construct a desired BS state, a calculation on the high-spin (HS) state is first completed, which is a pure spin state described by a single determinant, with all unpaired electrons aligned in the same direction (spin up) to adopt the highest possible total spin state *S*. For the $Mo^{4+}6Fe^{2+}1Fe^{3+}$ oxidation state, the high-spin state has the total spin $S = {}^{29}/_{2}$; for $Mo^{4+}4Fe^{2+}3Fe^{3+}$, the corresponding high-spin state is $S = {}^{31}/_{2}$. The density of the HS state was then flipped, by exchanging designated blocks of alpha and beta electron densities (from the fit electron density in ADF). In this way, the starting density for the desired spin-flipped $S = {}^{3}/_{2} = M^{N}$ resting state and $S = 1 = M^{OX}$ one-electron oxidized state were created, from which BS states were obtained. All calculations used the BS6-1 spin coupling alignment for FeMoco, defined in previous papers[3] as the spin coupling alignment that gave an electronic structure for the cofactor consistent with experimental observations. The $S = 1 = M^{OX}$ state was

(3) (a) Lovell, T.; Li, J.; Liu, T.; Case, D. A.; Noodleman, L. *J. Am. Chem. Soc.* **2001**, *123*, 12392. (b) Lovell, T.; Li, J.; Case, D. A.; Noodleman, L. *J. Am. Chem. Soc*. **2002**, *124*, 4546. (c) Lovell, T.; Torres, R. A.; Han, W.-G.; Liu, T.; Case, D. A.; Noodleman, L. *Inorg. Chem*. **2002**, *41*, 5744. (d) Lovell, T.; Li, J.; Case, D. A.; Noodleman, L. *J. Biol. Inorg. Chem*. **2002**, *7*, 735.

(4) (a) Deng, H.; Hoffmann, R. *Angew. Chem., Int. Ed. Engl.* **1993**, *32*, 1062. (b) Stavrev, K. K.; Zerner, M. C. *Chem.—Eur. J.* **1996**, *2*, 83. (c) Stavrev, K. K.; Zerner, M. C. *Theor. Chim. Acta* **1997**, *96*, 141. (d) Stavrev, K. K.; Zerner, M. C. *Int. J. Quantum Chem*. **1998**, *70*, 1159. (e) Dance, I. *Aust. J. Chem*. **1994**, *47*, 979. (f) Dance, I. *Chem. Commun*. **1997**, 165. (g) Dance, I. *Chem. Commun*. **1998**, 523. (h) Dance, I. *J. Biol. Inorg. Chem*. **1996**, *1*, 581. (i) Siegbahn, P. E. M.; Westerberg, J.; Svensson, M.; Crabtree, R. H. *J. Phys. Chem. B* **1998**, *102*, 1615. (j) Rod, T. H.; Hammer, B.; Nørskov, J. K. *Phys. Rev. Lett*. **1999**, *82*, 4054. (k) Rod, T. H.; Logadottir, A.; Nørskov, J. K. *J. Chem. Phys*. **2000**, *112*, 5343. (l) Rod, T. H.; Nørskov, J. K. *J. Am. Chem. Soc*. **2000**, *122*, 12751. (m) Szilagyi, R. K.; Musaev, D. K.; Morokuma, K. *Inorg. Chem*. **2001**, *40*, 766. (n) Durrant, M. C. *Inorg. Chem. Commun*. **2001**, *4*, 60. (o) Barriere, F.; Pickett, C. J.; Talarmin, J. *Polyhedron* **2001**, *20*, 27. (p) Durrant, M. C. *Biochem. J*. **2001**, *355*, 569. (q) Durrant, M. C. *Biochemistry* **2002**, *41*, 13946. (r) Durrant, M. C. *Biochemistry* **2002**, *41*, 13934.

(5) (a) Lee, H.-I.; Hales, B. J.; Hoffman, B. M. *J. Am. Chem. Soc*. **1997**, *119*, 11395. (b) True, A. E.; Nelson, M. J.; Venters, R. A.; Orme-Johnson, W. H.; Hoffman, B. M. *J. Am. Chem. Soc*. **1988**, *110*, 1935.

(6) Yoo, S. J.; Angove, H. C.; Papaefthymiou, V.; Burgess, B. K.; Munck, E. *J. Am. Chem. Soc*. **2000**, *122*, 4926.

(7) (a) Torres, R. A.; Lovell, T.; Noodleman, L.; Case, D. A. *J. Am. Chem. Soc*. **2003**, *125*, 1923 and references therein. (b) Ullmann, G. M.; Noodleman, L.; Case, D. A. *J. Biol. Inorg. Chem.* **2002**, *7*, 623.

(8) *ADF 2.3.0*; Department of Theoretical Chemistry, Free University of Amsterdam: Amsterdam, 1997.

(9) (a) Snijders, J. G.; Baerends, E. J.; Vernooijs, P. *At. Nucl. Data Tables* **1982**, *26*, 483. (b) Vernooijs, P.; Snijders, J. G.; Baerends, E. J. *Slater Type Basis Functions for the Whole Periodic System*; Internal report; Free University of Amsterdam: Amsterdam, The Netherlands, 1981. (c) Krijn, J.; Baerends, E. J. *Fit Functions in the HFS-method*; Internal report (in Dutch); Free University of Amsterdam: Amsterdam, The Netherlands, 1984.

(10) (a) Boerrigter, P. M.; te Velde, G.; Baerends, E. J. *Int. J. Quantum Chem*. **1988**, *33*, 87. (b) te Velde, G.; Baerends, E. J. *J. Comput. Phys*. **1992**, *99*, 84.

(11) (a) Versluis, L.; Ziegler, T. *J. Chem. Phys*. **1988**, *88*, 322. (b) Schlegel, H. B. In *Ab initio Methods in Quantum Chemistry-I*; Lawley, K. P., Ed.; Advances in Chemical Physics, Vol. 67; Wiley: New York, 1987.

(12) (a) Vosko, S. H.; Wilk, L.; Nusair, M. *Can. J. Phys*. **1980**, *58*, 1200. (b) Perdew, J. P.; Chekavry, J. A.; Vosko, S. H.; Jackson, K. A.; Perderson, M. R.; Singh, D. J.; Fioihais, C. *Phys. Rev. B* **1992**, *46*, 6671. (c) Becke, A. D. *J. Chem. Phys*. **1986**, *84*, 4524.

(13) Intramolecular proton transfer from the second shell hydrogen bonding partners and the oxygen ends of the homocitrate ligand did not occur.

(14) Noodleman, L. *J. Chem. Phys*. **1981**, *74*, 5737.

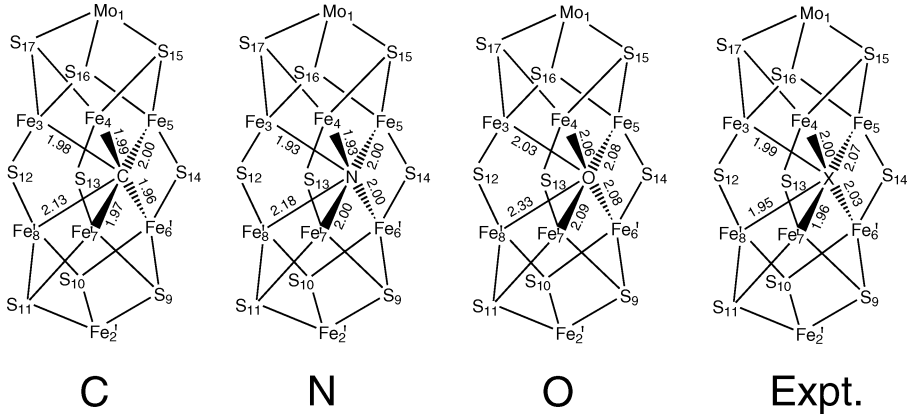

Figure 2. Fe−X distances (Å) calculated for the FeMocoX (X = C^{4-}, N^{3-}, or O^{2-}) core. Distances are shown at the $Mo^{4+}4Fe^{2+}3Fe^{3+}$ oxidation level.

Table 1. Averaged Bond Distances (Å) of the FeMocoX (X = C^{4-}, N^{3-}, O^{2-}) Cores[a]

	$6Fe^{2+}Fe^{3+}$				$4Fe^{2+}3Fe^{3+}$				
bond type	C	N	O	vacancy	C	N	O	vacancy	expt
Mo−Fe	2.81	2.80	2.80	2.75	2.77	2.78	2.81	2.75	2.70
Fe−Fe	2.63	2.69	2.76	2.70	2.64	2.65	2.79	2.64	2.61
Fe−X[b]	2.02	2.03	2.17		2.01	2.02	2.11		2.00
Fe−Fe′	2.63	2.67	2.82	2.75	2.61	2.63	2.74	2.66	2.59
Fe′−Fe′	2.76	2.71	2.75	2.70	2.70	2.69	2.74	2.66	2.66

[a] All calculations carried our for spin coupled state BS6-1 defined previously.[3] [b] Fe−X is the average of all six coordinated Fe−X and Fe′−X distances.

obtained from the $S = {}^3/_2 = M^N$ state by removing one electron of majority spin and optimizing the geometry.

2.3. Redox Potential Calculations. Redox potentials were calculated using methodology developed and applied previously to manganese and iron superoxide dismutases,[15] as well as iron−sulfur clusters.[3,7,16] Single step Poisson−Boltzmann calculations were performed for the interaction of the quantum cluster with the protein solvent environment as specified in ref 3d. Electrostatic potential charges were used to represent the charge distribution of the quantum cluster. For the resting FeMoco, the calculated redox potential has been shown to be insensitive to the choice of the spin state for the one-electron oxidized FeMoco. Consequently, only the redox event from the $S = {}^3/_2 = M^N$ state to the $S = 1 = M^{OX}$ state has been examined here, as redox transitions to the other possible states for M^{OX} ($S = 0$ or 2) have been shown to yield results that do not differ significantly.[3d]

2.4. Isomer Shift Calculations. Using all-electron DFT calculations, we have used a previously constructed linear correlation of measured Mössbauer isomer shifts with computed total s electron density for a variety of 1Fe, 2Fe, and 4Fe sulfur complexes to compare calculated isomer shifts of the FeMoco with those measured experimentally.[3a] The standard deviation for these fits varied between 0.05 and 0.06 mm s^{-1}, while correlation coefficients varied from $r = -0.94$ to -0.95.

3. Results

3.1. Comparison Modeling of the Bond Distances of the Central Core. On the basis of the resolution-dependent electron-density profiles, the central atom of FeMoco has been proposed to be C, N, or O.[1] Calculated core structures for C^{4-}, N^{3-}, and O^{2-} anions in the center of the FeMoco are given in Figure 2 and Table 1, along with the structural data at a resolution of 1.16 Å. A comparison of the structural data with the calculated parameters indicates that oxygen is improbable as Fe−O bond distances are calculated to be much longer than in the X-ray structural data. The FeMoco cluster therefore expands too much when a single O^{2-} anion is present. Interestingly, we have also tried to place molecules such as OH^-, H_2O, and NH^{2-} in the center of the cluster, and the FeMoco also expands substantially. Therefore, consistent with experimental analysis,[1] we discount diatomic or solvent molecules also. Both N^{3-} and C^{4-} produce Fe−N and Fe−C distances in reasonable accord with the X-ray data, and we cannot discriminate between them solely on the basis of the calculated structures. It is also worth noting that compared to our previous calculations, where calculated Fe−Fe distances were longer than experiment when there was no central anion, the Fe−Fe distances across the central waist contract slightly when a C^{4-} or an N^{3-} anion is present. The presence of the central atom would appear to play an important geometric role in constraining the 6Fe prismane core.

The X-ray data[1] suggest that the central atom sits fairly equally displaced in the 6Fe prism. All Fe sites therefore now appear to be four coordinate and no longer display the unusual trigonal coordination, as was suggested originally. Our calculations indicate that the N^{3-} anion lies closer to sites Fe3 and Fe4, rather than being equally displaced between all six irons of the core. An asymmetrically located central atom was also observed in recent calculations of the protonated and reduced states of the FeMoco.[3b] Here, a single proton sitting in the central cavity also favored site Fe4. However, in both cases, the same spin coupling pattern was used in the calculations. It is likely that the position of the N^{3-} anion and the resultant Fe−N bond distances arise due to the specific pattern of up and down majority site spin vectors employed and that the pattern of Fe−N bond distances will vary in accord with the spin coupling pattern.

Calculations for the FeMoco at the two most probable resting oxidation states, $Mo^{4+}4Fe^{2+}3Fe^{3+}$ and $Mo^{4+}6Fe^{2+}1Fe^{3+}$, give similar structural trends, in that O^{2-} seems unlikely to be the central ligand due to a larger overall geometric expansion of the cluster, while C^{4-} and N^{3-} cannot be distinguished by bond length comparisons with the X-ray data alone. The more oxidized $Mo^{4+}4Fe^{2+}3Fe^{3+}$ state shows a slight contraction both in FeMoco cluster size and in Fe−X (X = C^{4-}, N^{3-}, or O^{2-}) distances relative to the $Mo^{4+}6Fe^{2+}1Fe^{3+}$ reduced state, and in that sense, there is a small improvement in overall geometric correlation with the 1.2 Å structure for the more oxidized assignment of metal-ion valencies.

On the basis of the resolution-dependent electron-density profile and the fact that nitrogenase interacts with dinitrogen to

(15) Han, W.-G.; Lovell, T.; Noodleman, L. *Inorg. Chem.* **2002**, *41*, 205.
(16) Li, J.; Nelson, M. R.; Peng, C. Y.; Bashford, D.; Noodleman, L. *J. Phys. Chem. A* **1998**, *102*, 6311.

Table 2. Calculated Redox Potentials for Redox Transition (Oxidized FeMoco + e^- → Resting FeMoco)

redox transition[a]	charge changes on redox[b]	I.P. (eV)	ΔE_{pr} (eV)	redox potential (eV)
$Mo^{4+}5Fe^{2+}2Fe^{3+}N^{3-} + e^- \rightarrow Mo^{4+}6Fe^{2+}1Fe^{3+}N^{3-}$	$-6 + -1 \rightarrow -7$	−10.35	+12.56	−2.21
$Mo^{4+}3Fe^{2+}4Fe^{3+}C^{4-} + e^- \rightarrow Mo^{4+}4Fe^{2+}3Fe^{3+}C^{4-}$	$-5 + -1 \rightarrow -6$	−8.49	+11.61	−1.31
$Mo^{4+}3Fe^{2+}4Fe^{3+}N^{3-} + e^- \rightarrow Mo^{4+}4Fe^{2+}3Fe^{3+}N^{3-}$	$-4 + -1 \rightarrow -5$	−5.34	+9.96	+0.19
$Mo^{4+}5Fe^{2+}2Fe^{3+} + e^- \rightarrow Mo^{4+}6Fe^{2+}1Fe^{3+}$	$-3 + -1 \rightarrow -4$	−2.52	+7.76	+0.82
$Mo^{4+}3Fe^{2+}4Fe^{3+}O^{2-} + e^- \rightarrow Mo^{4+}4Fe^{2+}3Fe^{3+}O^{2-}$	$-3 + -1 \rightarrow -4$	−2.45	+7.85	+0.97
$Mo^{4+}3Fe^{2+}4Fe^{3+} + e^- \rightarrow Mo^{4+}4Fe^{2+}3Fe^{3+}$	$-1 + -1 \rightarrow -2$	+2.08	+3.65	+1.30
expt				−0.042[c]

[a] All redox potentials calculated using ΔE°_{redox} = I.P. + ΔE_{pr} − 4.43.[3,7,16] [b] For comparison with the P cluster of the same protein, omitting or neutralizing the carboxylates of the homocitrate would change the charge on FeMoco by +2 in each case. [c] Measured for *A. vinelandii*.[18]

make ammonia, Einsle *et al.*[1] proposed that it was reasonable to assign the central ligand as a nitrogen atom. Recently, plane-wave DFT calculations by Hinnemann and Nørskov and DMol calculations by Dance[17] also examined the various possibilities that the light element in the center of the cofactor could be carbon, nitrogen, or oxygen. Comparing those works with our own, there are some relevant differences in approach. Hinnemann and Nørskov considered a smaller active site model in the gas phase only and compensated for the additional charge of the central X ligand (X = C^{4-}, N^{3-}, or O^{2-}) by an equal number of protons on the cluster sulfurs (and on Fe for C^{4-}). By contrast, we have performed calculations on a larger active site model for which the central anion increases the cluster's negative charge compared to a central vacancy model, and energetics are assessed by redox potential calculations in the protein and solvent environment. After consideration of the O and N possibilities, Dance, as well as Hinnemann and Nørskov, suggested the most likely resting state for an atom-centered FeMoco was $Mo^{4+}4Fe^{2+}3Fe^{3+}(\mu_6\text{-}N^{3-})$. Nevertheless, the results of Hinnemann and Nørskov's and Dance's calculations, which were favorable for a nitride anion from both a structural and energetic perspective, agree structurally with that presented here and add support to the crystallographic assignment.

3.2. Redox Potential Calculations. In Table 2, calculated redox potentials in the protein environment are presented for the interconversion between two states of the FeMoco, from the resting $S = {}^3/_2 = M^N$ state to a state that is one-electron oxidized $S = 1 = M^{OX}$ relative to the resting enzyme. Calculated redox data are presented for several independent processes that could represent the observed redox event, FeMoco(oxidized) + e^- → FeMoco(resting), along with the measured value of −0.042 V in *Azotobacter vinelandii*.[18]

In a previous paper,[3d] using the metal-ion valence assignments based on the ENDOR data,[5] we reported the calculated redox potential for the process, $Mo^{4+}5Fe^{2+}2Fe^{3+} + e^- \rightarrow Mo^{4+}6Fe^{2+}1Fe^{3+}$, to be +0.82 eV. Based on metal-ion valence assignments from Mössbauer data, the more oxidized redox potential, described by $Mo^{4+}3Fe^{2+}4Fe^{3+} + e^- \rightarrow Mo^{4+}4Fe^{2+}3Fe^{3+}$, was calculated to be +1.30 eV. Since those previous efforts to calculate the redox potential, we have tried several different approaches to obtain a more accurate value. These have included calculations of FeMoco with a deprotonated imidazole ring bound to molybdenum, exploring coupled redox events involving protons on the homocitrate or the imidazole ring and electrons on the molybdenum−iron cluster, incorporating different protonation states of the surrounding protein amino acid side chains, and variations in the density functional and electrostatics methodology employed. None of these approaches reproduced the observed redox potential within an error margin of a few tenths of an electron volt. After discussing potential problems with the calculations, we concluded that "*there may be additional structural uncertainties even in the current fairly high-resolution structures.*"[3d] While we cannot claim to have predicted the existence of a central ligand, the fact that the wrong structure yielded a very poor calculated redox potential supports the utility of quantitative redox potential calculations as a "reality" check for models of metalloprotein active sites.

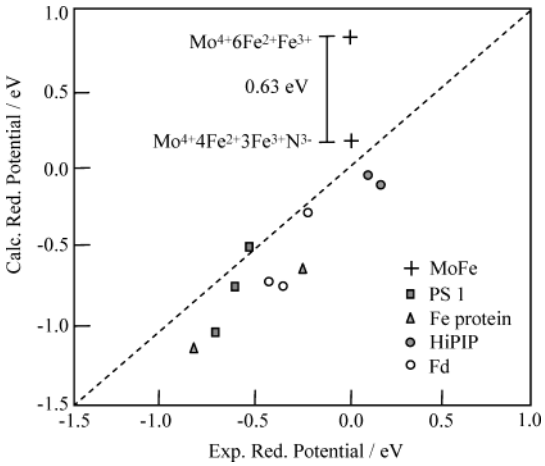

Figure 3. Plot of calculated FeMoco redox potential versus experiment. For comparison, redox potentials calculated for a range of iron−sulfur proteins (see ref 7a) are shown.

The incorporation of an N^{3-} anion in the center of the FeMoco now gives us a chance to evaluate this finding energetically with respect to the redox data. From Table 2, it is immediately clear that the redox process described by $Mo^{4+}3Fe^{2+}4Fe^{3+}N^{3-} + e^- \rightarrow Mo^{4+}4Fe^{2+}3Fe^{3+}N^{3-}$, calculated to be +0.19 eV, although not perfect, is in much better agreement with the experimental value. This contrasts with that for the redox process described by $Mo^{4+}5Fe^{2+}2Fe^{3+}N^{3-} + e^- \rightarrow Mo^{4+}6Fe^{2+}1Fe^{3+}N^{3-}$, where the calculated value of −2.2 V is far too negative. Our new calculated value for the FeMoco redox process, in which $Mo^{4+}4Fe^{2+}3Fe^{3+}N^{3-}$ are the favored valence assignments in the resting state, is much improved over the previous assignment of $Mo^{4+}6Fe^{2+}1Fe^{3+}$ with a central vacancy, and as can be seen in Figure 3, this value now falls more in line with the results of redox potentials we have calculated for other iron−sulfur proteins.

As noted previously, although oxygen is unlikely as a central ligand, we were unable to rule out a carbon anion on the basis

(17) (a) Hinnemann, B.; Norskov, J. K. *J. Am. Chem. Soc.* **2003**, *125*, 1466. (b) Dance, I. *Chem. Commun.* **2003**, 324.
(18) O'Donnell, M. J.; Smith, B. E. *Biochem. J.* **1978**, *173*, 831.

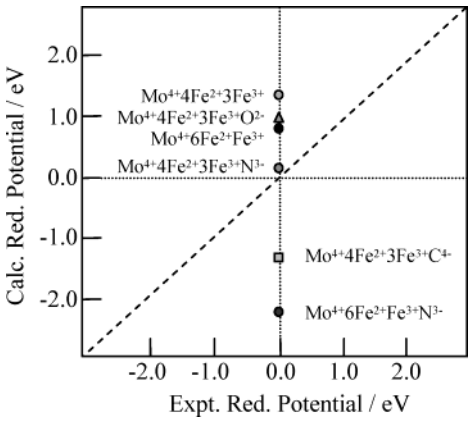

Figure 4. Correlation of calculated versus experimental redox potential for the FeMoco. Points in the upper left quadrant arise from FeMoco cluster charge changes ranging −1 to −5; those in the lower right quadrant derive from charge changes ranging −5 to −7.

Table 3. Gas Phase and Protein Interaction Energies for FeMoco Oxidation States

oxidation states	total charge[a]	gas phase (eV)	E_{pr} (eV)
$6Fe^{2+}1Fe^{3+}N^{3-}$	−7	−411.7835	−54.85
$5Fe^{2+}2Fe^{3+}N^{3-}$	−6	−422.1369	−42.29
$4Fe^{2+}3Fe^{3+}N^{3-}$	−5	−430.6144	−31.09
$3Fe^{2+}4Fe^{3+}N^{3-}$	−4	−435.9511	−21.13
$6Fe^{2+}1Fe^{3+}$	−4	−426.6996	−20.92
$5Fe^{2+}2Fe^{3+}$	−3	−429.2124	−13.10
$4Fe^{2+}3Fe^{3+}$	−2	−428.7386	−7.46
$3Fe^{2+}4Fe^{3+}$	−1	−426.6522	−3.81

[a] For comparison with the P cluster of the same protein, omitting or neutralizing the carboxylates of the homocitrate would change the charge on FeMoco by +2 in each case.

of Fe−C distances alone, as they were effectively indistinguishable from the Fe−N distances observed both in the geometry optimizations and in the high-resolution X-ray data. In this context, we have also evaluated the redox potentials for the FeMoco clusters with O^{2-} and C^{4-} in the center at the Mo^{4+}-$4Fe^{2+}3Fe^{3+}$ level. Along with the redox data for the FeMoco models with a central N^{3-} anion, these are shown in Table 2 and Figure 4. The most striking feature of Figure 4 is that the redox potential calculated for $Mo^{4+}3Fe^{2+}4Fe^{3+}C^{4-} + e^- \rightarrow Mo^{4+}4Fe^{2+}3Fe^{3+}C^{4-}$, at −1.31 eV, is far too negative; that for $Mo^{4+}5Fe^{2+}2Fe^{3+}O^{2-} + e^- \rightarrow Mo^{4+}6Fe^{2+}1Fe^{3+}O^{2-}$ is too positive.

Along with the geometric criteria, these calculated redox values further enable us to discount both O and C as the central anion (as Einsle *et al.*[1] did previously on the basis of their chemical intuition). More importantly, these incorrect redox potentials for O and C in the center of the FeMoco illustrate the usefulness of redox potential calculations in providing an energetic measure of the correctness of structure.

The calculated potentials in Table 2 are clearly dependent on the total charges associated with the two FeMoco clusters involved in the redox event. As these clusters become progressively more negatively charged, so too do the calculated redox and ionization potentials; the change in the environmental contribution (ΔE_{pr}) to the redox process also increases with increasing negative charge. If we consider when only the N^{3-} anion is present in Table 3, as electrons become removed from the FeMoco, the cluster stabilizes due to a larger number of ferric−ferric pairs and the increased single-ion exchange energy associated with the ferric sites. As the resting FeMoco becomes increasingly more reduced, the total charge on the cofactor increases from −5 to a maximum of −7 and the interaction energy of the cofactor with the protein and solvent environment increases dramatically. It therefore appears that it is the interplay of these two competing terms that regulates the calculated redox potentials, and in this respect, assigning the correct charge to the FeMoco cluster is essential to properly describe the redox energetics.

Furthermore, the trend in redox potential as a function of the cofactor charge enables us to estimate the redox potential for a variety of oxidation states and central ligands. For example, the redox process described by $Mo^{4+}5Fe^{2+}2Fe^{3+}O^{2-} + e^- \rightarrow Mo^{4+}6Fe^{2+}1Fe^{3+}O^{2-}$ involves changes in charge of $-5 + -1 \rightarrow -6$. By comparison with redox potentials of the same charges in Table 2, the calculated redox potential should therefore be around −1.3 eV. For $Mo^{4+}5Fe^{2+}2Fe^{3+}C^{4-} + e^- \rightarrow Mo^{4+}6Fe^{2+}1Fe^{3+}C^{4-}$, intrinsic cluster charges of $-7 + -1 \rightarrow -8$ must yield a redox potential that is much more negative than −2.2 eV. Both values are sufficiently far removed from the experimental value of −42 mV in *Azotobacter vinelandii* that they can be excluded.

Another potential class of models would involve a more reduced $Mo^{4+}6Fe^{2+}Fe^{3+}$core with a central atom (C, N, O), but with the extra charge compensated for by protonation, most probably at the μ^2S atoms. The two clearest examples of this would involve an O^{2-} or N^{3-} as the central anion and one or two added protons, respectively. Both models would exhibit the same overall total cluster charge of −5. As similarly charged clusters are likely to give comparable redox potentials, the predicted redox potentials should also prove to be around +0.2 eV, as was found for $Mo^{4+}4Fe^{2+}3Fe^{3+}N^{3-}$ without the protons (Table 2 and Figure 4). Such models may also be viable candidates for the resting FeMoco.

As a further test, we have also examined the geometry of the $Mo^{4+}6Fe^{2+}Fe^{3+}O^{2-}H^+$ core, shown in Figure 5, along with its unprotonated $Mo^{4+}6Fe^{2+}Fe^{3+}O^{2-}$ counterpart, the experimental structure, and our calculated structure of $Mo^{4+}4Fe^{2+}3Fe^{3+}N^{3-}$. For the $Mo^{4+}6Fe^{2+}Fe^{3+}O^{2-}$ core, although Fe−μ^2S distances of 2.26 Å on average agree reasonably well with those of the X-ray structure (2.22 Å), longer average Fe−Fe′ (2.82 Å) and Fe−O (2.17 Å) distances, along with its redox potential (estimated on the basis of charge to be about −1.3 eV), make it an unlikely option. By protonating one of the μ^2S atoms, as noted previously, the charge on the cluster would seem to be right to give a reasonable redox potential. However, then the two Fe−μ^2S(H) bonds lengthen to 2.35 and 2.38 Å, much longer than the other four Fe−μ^2S bonds, which range 2.23−2.25 Å. The equivalent bonds in the X-ray data display a range of 2.17−2.26 Å and an average of 2.22 Å, which are consistent with no protonation. Calculated Fe−O (2.11 Å) and Fe−Fe′ (2.87 Å) distances are also longer on average than the equivalent experimental distances of 2.00 and 2.59 Å. Structurally, the $Mo^{4+}6Fe^{2+}Fe^{3+}O^{2-}H^+$ core is much poorer than our best model of $Mo^{4+}4Fe^{2+}3Fe^{3+}N^{3-}$, which displays *both* geometric ($Fe-\mu^2S_{av} = 2.23$ Å, $Fe-N_{av} = 2.02$ Å, $Fe - Fe'_{av} = 2.63$ Å) and redox (+0.19 eV) features consistent with experiment. A doubly protonated $Mo^{4+}6Fe^{2+}Fe^{3+}N^{3-}2H^+$ model would therefore also be unlikely, as it would be expected to give similar or larger Fe−Fe′ and Fe−μ^2S distances compared to the $Mo^{4+}6Fe^{2+}Fe^{3+}O^{2-}H^+$ core.

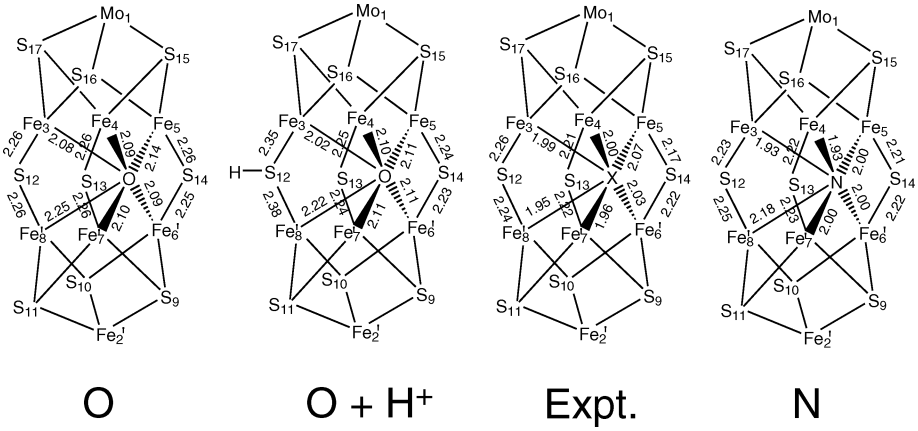

Figure 5. Fe−S and Fe−X distances (Å) calculated for FeMocoX (X = O^{2-} and N^{3-}) cores. From left to right, molecules correspond to $Mo^{4+}6Fe^{2+}Fe^{3+}O^{2-}$, $Mo^{4+}6Fe^{2+}Fe^{3+}O^{2-}H^{+}$, the 1.2 Å X-ray structure,[1] and $Mo^{4+}4Fe^{2+}3Fe^{3+}N^{3-}$.

Table 4. Calculated ^{57}Fe Isomer Shifts (mm s^{-1}) for the FeMoco Cluster

oxidation state	total charge[a]	range	average
$6Fe^{2+}1Fe^{3+}N^{3-}$	−7	0.49−0.62	0.54
$4Fe^{2+}3Fe^{3+}N^{3-}$	−5	0.41−0.60	0.48
$6Fe^{2+}{}^{+}1Fe^{3+}$	−4	0.21−0.40	0.30
$4Fe^{2+}3Fe^{3+}$	−2	0.10−0.35	0.24
expt		0.33−0.50	0.40[b]

[a] All isomer shifts were derived from a linear fit (−0.51(nuclear density − 11890.0) + 0.36) of 1Fe, 2Fe, and 4Fe S-phenyl and S_2-*o*-xylyl group model compounds to iron−sulfur protein isomer shift data.[3a] [b] Measured at 4.2 K for resting state of enzyme ($S = {}^3/_2$).[6]

Table 5. Calculated Net Spin Density for the Central Anion of FeMoco

FeMoco model	net spin density
$Mo^{4+}4Fe^{2+}3Fe^{3+}C^{4-}$	−0.14
$Mo^{4+}4Fe^{2+}3Fe^{3+}N^{3-}$	−0.02
$Mo^{4+}4Fe^{2+}3Fe^{3+}O^{2-}$	−0.01

3.3. Isomer Shift Calculations. Table 4 reports experimental isomer shift data, along with calculated isomer shift values for FeMoco for the two postulated oxidation state assignments, in both the absence and the presence of the multiply charged N^{3-} ion in the center of the cofactor. Also reported is the total cluster charge for each set of oxidation state assignments.

Previously, for FeMoco with no central N^{3-} anion,[3a] the more reduced $Mo^{4+}6Fe^{2+}1Fe^{3+}$ oxidation state assignment was calculated to have an average isomer shift value of 0.30 mm s^{-1}; the corresponding value for the $Mo^{4+}4Fe^{2+}3Fe^{3+}$ metal-ion valence assignments was 0.24 mm s^{-1}. On the basis of the experimentally reported average of 0.40 mm s^{-1}, we concluded that the $Mo^{4+}6Fe^{2+}1Fe^{3+}$ oxidation state assignment was more likely to be correct. With the revised model that now incorporates the central N^{3-} anion, the calculated average isomer shift for $Mo^{4+}4Fe^{2+}3Fe^{3+}$ is 0.48 mm s^{-1}, closer to an average experimental value of 0.40 mm s^{-1}. By contrast, the $Mo^{4+}6Fe^{2+}$-$1Fe^{3+}$ oxidation state assignment is now calculated to give an average isomer shift value of 0.54 mm s^{-1} and an error of 0.14 mm s^{-1}.

The trend in calculated isomer shift values is exactly what one would expect given electron counting arguments and charge transfer from nitride to iron. With no central N^{3-} anion, the ENDOR-based $Mo^{4+}6Fe^{2+}1Fe^{3+}$ valence assignments result in a cofactor with total charge of −4, and based on a comparison of calculated and observed average isomer shift values, our original conclusion was that the cofactor was electron deficient. Oxidation of two of the ferrous sites to ferric yielded the $Mo^{4+}4Fe^{2+}3Fe^{3+}$ model, which made the cofactor total charge −2 and rendered the cofactor even more electron deficient, such that the calculated average isomer shift values were further from those measured experimentally. The subsequent addition of the nitride ion, having a charge of −3, offsets the oxidation of two ferrous sites and also reduces the cofactor net charge by one extra negative unit, giving a cluster with an overall total charge of −5. The qualitative conclusion to be drawn is that although the new $Mo^{4+}4Fe^{2+}3Fe^{3+}N^{3-}$ model is formally two electrons more oxidized than the original $Mo^{4+}6Fe^{2+}1Fe^{3+}$ model in terms of valence assignments of the iron sites, due to the addition of N^{3-}, the cofactor is, in fact, one electron more reduced overall. The seven iron sites must therefore be electron rich relative to the original ENDOR-based model, and this enables us to rationalize the trend in calculated average isomer shift in Table 4. However, it is also worth noting that, in the protein environment around FeMoco, there are several amino acid residues lying close to the FeMoco that could easily accept charge donation from the cluster.[2,3d] These residues are not included in our quantum chemical model but could well be the reason that our calculated average isomer shift data suggest the cluster is now somewhat too electron rich.

Overall, these new isomer shift estimates suggest that the oxidation state assignment of $Mo^{4+}4Fe^{2+}3Fe^{3+}N^{3-}$ is more compatible with experiment, and a more reduced $Mo^{4+}6Fe^{2+}1Fe^{3+}N^{3-}$ cluster assignment is not required.

3.4. Spin Density Associated with the Central Ligand. In Table 5, calculated Mulliken net spin densities are given for FeMoco clusters with C, N, or O in the center. The total net spin density on these central anions is very small for N^{3-} and O^{2-} but larger for C^{4-}. The calculated magnitude of the N^{3-} spin population is −0.02 of an electron, further broken down into total *s* (0.02) and total *p* (−0.04) contributions (where $p_x + p_y + p_z = 0.01 + -0.05 + 0.00$). This spin density distribution would give rise to an ^{14}N hyperfine signal that may be difficult to observe or identify,[19] especially when one considers that FeMoco is hydrogen bonded to several amino acid side chains and main chain peptides derived from arginine,

(19) Lee, H.-I.; Thrasher, K. S.; Dean, D. R.; Newton, W. E.; Hoffman, B. M. *Biochemistry* **1998**, *37*, 13370.

glycine, and lysine, making the local protein environment relatively nitrogen rich, and all of which may mask any potential spectroscopic signal. Lee et al.[20] have recently observed no new ^{15}N signals or changes in ^{14}N hyperfine spectra during ENDOR and ESEEM experiments under catalytic turnover with $^{15}N_2$. This is consistent with a stable central ligand that is not exchangeable, which argues against the dinitrogen substrate being the source of a central N.

4. Summary

Quantum chemical calculations have been used to examine which of three proposed atoms, C, N, or O, is present in the center of the active site of nitrogenase. The calculations yield structural, spectroscopic, and energetic evidence to corroborate the hypothesis that the central atom sitting in the six-iron prismane of the FeMoco is an N^{3-} anion, as was suggested recently by Rees and co-workers and further reinforced by theoretical studies.[17] We also reach this conclusion on the basis of calculated Fe−N bond distances that are in very good agreement with the high-resolution X-ray data, a calculated redox potential of 0.19 eV that compares well with the experimental value of −0.042 V in the protein, for the process defined as $M^{OX} + e^- \rightarrow M^N$, or, in oxidation state terms, $Mo^{4+}3Fe^{2+}4Fe^{3+} + e^- \rightarrow Mo^{4+}4Fe^{2+}3Fe^{3+}$ and isomer shift calculations that suggest a metal-ion valence assignment of $Mo^{4+}4Fe^{2+}3Fe^{3+}$ for the resting state. Furthermore, in the presence of the N^{3-} anion, the homocitrate anion is stable in the $Mo^{4+}4Fe^{2+}3Fe^{3+}$ state; our earlier DFT calculations with a central vacancy[3a] produced spontaneous oxidation of the homocitrate to yield a terminal homocitrate radical, which is not observed experimentally.

The incorporation of a central N^{3-} anion into the FeMoco raises many questions about both the cluster assembly and the catalytic reaction mechanism. Some of the most significant questions include how does the N^{3-} anion become incorporated into the center of the FeMoco, does the N^{3-} anion play any role in the catalytic cycle, perhaps in initial dinitrogen binding, or does it mainly serve a structural and electronic role in maintaining the integrity of the cluster during catalysis? Molecular modeling is well suited to be able to tackle such questions, and such issues will be the focus of future studies in our laboratory.

Acknowledgment. This work was supported by NIH grant GM 39914. We also thank the theoretical chemistry group at the Free University of Amsterdam for the use of the ADF codes.

JA0301572

(20) Lee, H.-I.; Benton, P. M. C.; Laryukhin, M.; Igarashi, R. Y.; Dean, D. R.; Seefeldt, L. C.; Hoffman, B. M. *J. Am. Chem. Soc.* **2003**, *125*, 5604.